ChemComm

FEATURE ARTICLE

View Article Online
View Journal | View Issue

Cite this: *Chem. Commun.*, 2023, **59**, 1744

Propagating MOF flexibility at the macroscale: the case of MOF-based mechanical actuators

Javier Troyano *[ab] and Daniel Maspoch *[cde]

Shapeshifting materials have captured the imagination of researchers for their myriad potential applications, yet their practical development remains challenging. These materials operate by mechanical actuation: their structural responses to external stimuli generate mechanical work. Here, we review progress on the use of flexible metal–organic frameworks (MOFs) in composite actuators that shapeshift in a controlled fashion. We highlight the dynamic behaviour of flexible MOFs, which are unique among materials, even other porous ones, and introduce the concept of propagation, which involves the efficient transmission of flexible MOF deformations to the macroscale. Furthermore, we explain how researchers can observe, measure, and induce such effects in MOF composites. Next, we review pioneering first-generation MOF-composite actuators that shapeshift in response to changes in humidity, temperature, pressure, or to other stimuli. Finally, we allude to recent developments, identify remaining R & D hurdles, and suggest future directions in this field.

Received 26th October 2022,
Accepted 13th January 2023

DOI: 10.1039/d2cc05813h

rsc.li/chemcomm

[a] *Inorganic Chemistry Department, Autonomous University of Madrid, 28049 Madrid, Spain. E-mail: javier.troyano@uam.es*
[b] *Institute for Advanced Research in Chemical Sciences (IAdChem), Autonomous University of Madrid, 28049 Madrid, Spain*
[c] *Catalan Institute of Nanoscience and Nanotechnology (ICN2), CSIC and the Barcelona Institute of Science and Technology, Campus UAB, Bellaterra, 08193 Barcelona, Spain. E-mail: daniel.maspoch@icn2.cat*
[d] *Departament de Química, Facultat de Ciències, Universitat Autònoma de Barcelona, 08193 Bellaterra, Spain*
[e] *ICREA, Pg. Lluís Companys 23, 08010 Barcelona, Spain*

1. Introduction

In the quest to create shapeshifting systems, researchers have explored diverse classes of materials for use in mechanical actuators, devices whose structural response to external stimuli is converted into mechanical work. More than 2 decades ago, Kitagawa and co-workers predicted a third generation of metal–organic frameworks (MOFs), defining them as porous crystalline solids capable of reversibly undergoing structural changes in response to external stimuli.[2] Soon afterwards, they and

Javier Troyano

Javier Troyano received his PhD in Chemistry and Material Science at Autonomous University of Madrid in 2015. Then he worked as a Postdoctoral Researcher in Prof. Daniel Maspoch's group at Catalan Institute of Nanoscience and Nanotechnology (ICN2) in Barcelona (Spain). In 2019, he joined Prof. Shuhei Furukawa's group in iCeMS at Kyoto University (Japan) as a JSPS postdoctoral fellow. In 2022, he was awarded a María Zambrano grant from the Spanish Government and joined the Prof. Félix Zamora's group. His research mainly focuses on coordination and supramolecular chemistry at the macro and nanoscale for the design of novel functional materials.

Daniel Maspoch

Daniel Maspoch is an ICREA Research Professor at the Institut Català de Nanociència i Nanotecnologia (ICN2). He received his BS degree at the Universitat de Girona and his PhD degree at the Universitat Autònoma de Barcelona & Institut de Ciència de Materials de Barcelona. He worked as a postdoctoral fellow at Northwestern University. His research interests include reticular materials (MOFs, COFs and MOPs) and delivery systems.

other groups reported the first examples of MOFs exhibiting reversible structural transformations upon adsorption of guest molecules.[3,4] Since then, the list of flexible MOFs (also called soft porous crystals[5]) has steadily grown.[6,7] Research on flexible MOFs has led to the discovery of diverse response mechanisms based on variations in temperature,[3,8] light,[9–11] or mechanical stress,[12,13] and of fascinating phenomena such as negative thermal expansion,[14] negative gas-adsorption,[15] negative linear compressibility,[16] and shape-memory effect.[17]

The emergence of flexibility in MOFs can be explained by the combination of soft coordination bonds, weak intermolecular interactions, and the presence of internal voids, which provide more freedom for structural dynamics. Likewise, the high versatility in composition, topology, pore functionalisation, and crystal size/shape of MOFs all favour the diversity of possible structural transformations. Accordingly, much research is currently devoted to obtaining theoretical insight to understand the flexibility of MOFs and to develop tools for material design.[18–21]

The capacity of flexible MOFs to exhibit such a wide range of dynamic behaviour differs markedly from the case of conventional porous materials, which are typically rigid. Consequently, researchers have a unique vision of MOFs and their potential applications, as evidenced by reports published over the past decade.[6,22] For instance, flexible MOFs are excellent candidates for use in separation processes, exhibiting highly selective adsorption properties.[23] Another potential application of flexible MOFs lies in their ability to sense guest molecules.[24] Likewise, their capacity to capture/release guest molecules in response to an external stimulus makes them ideal vehicles for controlled drug delivery.[25]

Another way to harness the structural transformations of flexible MOFs is to exploit the mechanical stress generated by adsorption/desorption of guest molecules. Namely, when a flexible MOF experiences structural changes at the molecular scale, its crystal dimensions undergo mesoscale variations. Thus, if the generated stress is efficiently transferred, then a macroscale mechanical response can be obtained. Briefly, flexible MOFs can be employed to convert chemical energy into a mechanical response. Thus, over the past few years, researchers have created MOF-based mechanical actuators capable to change their shape in response to variations in environmental conditions. Mechanical actuators are materials that perform mechanical work by means of differential swelling/shrinking throughout a heterogeneous non-homogenous structure. Thus, the mismatch in the generated strain forces the actuator to adopt the most energetically-favourable shape. Importantly, to enable predictable shapeshifting, the swellable material must be properly distributed. In this sense, flexible MOFs are an ideal platform on which to develop shapeshifting materials. Unlike other kinds of materials used for creating soft actuators, such as polymeric films[26] or hydrogels,[27] MOFs are crystalline, thus offering the possibility to finely tune their porosities and morphologies, and consequently, their behaviour.

Here, we aim to review how the flexibility of MOFs can be transformed into useful work, introducing the recent progress on the development of MOF-based mechanical actuators. Firstly, we explain how researchers can observe and measure meso- and macroscale deformations in flexible MOFs that occur in response to external stimuli. The examples provide the basis for understanding the potential of flexible MOFs for creating autonomous soft materials. Next, we present the most relevant advances in the fabrication of the first flexible MOF-based actuators, discussing the pioneering work that has been done on asymmetric flexible-MOF composite films. Finally, we allude to recent developments, identify remaining R & D hurdles, and suggest future directions in this field, including the potential of porous materials analogous to MOFs.

2. Deformations of flexible MOFs across different length-scales

Among the main challenges for the practical application of flexible MOFs in mechanical actuation is to adapt their mechanical response to the required scale of work. In this sense, many of the potential applications of flexible MOFs can demand response at the macroscopic level, meaning that the MOF dynamics must be successfully transferred from the length-scale of individual crystals (mesoscale) to the macroscale. This concept, named as propagation, is not merely a question of translating the mechanical response to a larger scale but also involves establishing control over both the response time and the magnitude of the resultant deformation.

In this section, we outline how the events that lead to structural transformations at the molecular scale can be observed and quantified at the mesoscale, and used for operating at the macroscale.

2.1 Deformations of flexible MOF crystals: from the molecular to the mesoscopic scales

The development of methods for the characterisation of MOF structures have made enabled molecular studies of the structural transformations of flexible MOFs, whether on bulk solids or single crystals. However, only a few studies have addressed the effects of such transformations at the mesoscale, by analysing the morphological changes experienced by flexible MOF crystals. Pioneering studies in the 2000s first observed reversible macroscopic morphological changes in single MOF crystals using optical microscopy upon adsorption/desorption of solvent guest molecules.[28] However, it was not until the mid-2010s that these transformations began to be studied at the mesoscale. The first direct evidence of such mesoscopic shape changes was reported by Coronas *et al.*[29] With the help of an environmental scanning electron microscope (ESEM), they were able to track the geometric changes of a 1-micron-sized single crystal of MIL-53(Al) upon desorption, caused by the electron beam and subsequent temperature increase. Initially, MIL-53(Al) crystals were covalently attached to a glass support to correctly measure the temporal evolution in their shape. This strategy enabled the determination of the time-resolved extent of deformation of a single crystal (Fig. 1a). This work nicely illustrated how the

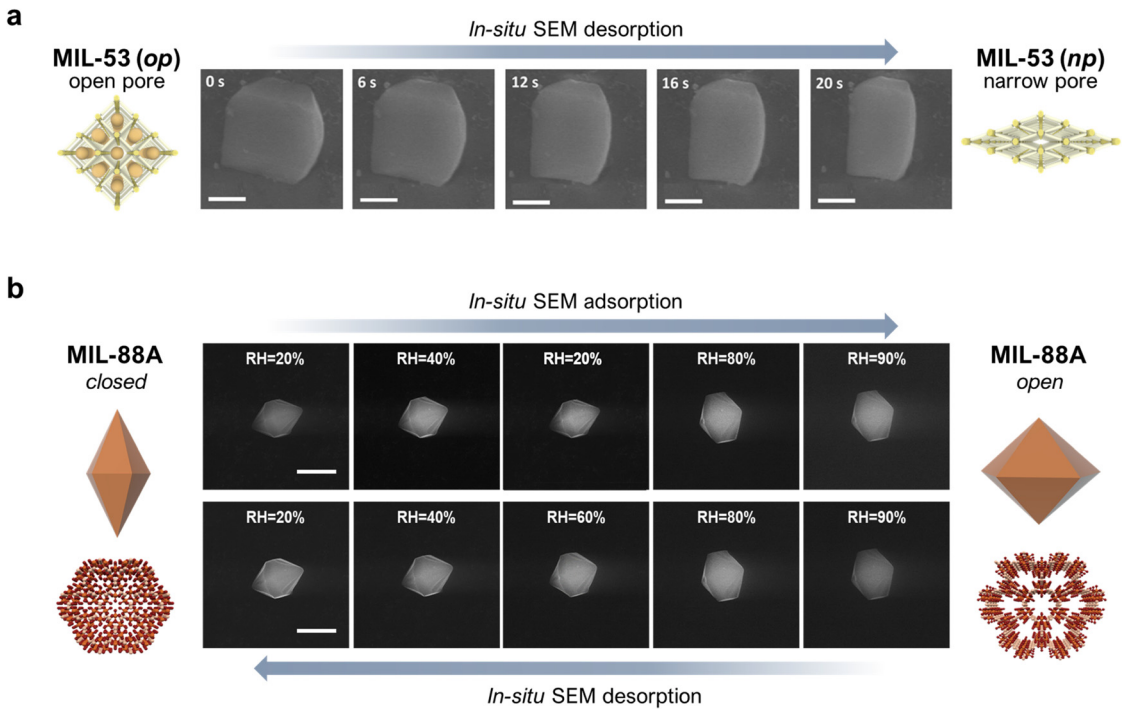

Fig. 1 (a) *In situ* FESEM images showing variations in the single-crystal dimensions of MIL-53(Al) over time. Scale bars = 500 nm. (b) *In situ*, humidity-controlled FESEM images of a single crystal of MIL-88A at different levels of relative humidity (RH). Top row: adsorption (from 20% RH up to 90% RH); Bottom row: desorption (from 90% RH back down to 20% RH). Scale bar = 5 μm. Adapted, with permission, from ref. 29 and 30.

effects of molecular transformations of flexible MOFs could be investigated at the mesoscale. However, it was limited to the analysis of the kinetics of single-crystal shape changes upon desorption. Taking this work as a reference, our group (the Maspoch group) later explored the use of a humidity-controlled ESEM for studying the geometric changes in a 1-micron-sized single crystal of MIL-88A (Fe) upon adsorption/desorption of water in near-equilibrium conditions.[30] As depicted in Fig. 1b, as the relative humidity (RH) increased from 20% to 90%, corresponding to the adsorption phase, the crystal length gradually decreased (~18%) and its width increased (~33%), leading to an overall increase of ~45% in crystal volume at 90% relative humidity. These results matched with the previously described structural transformation of MIL-88A, whereby for each cell, the *a*-parameter gradually increases while the *c*-parameter decreases. Likewise, when the relative humidity dropped back down to 20%, corresponding to the desorption phase, the crystal recovered its initial dimensions, which confirmed the reversibility of the adsorption/desorption (*i.e.* swelling/shrinkage) process. This work not only provided a full picture of the morphologic changes undergone by a single crystal of a flexible MOF, but also enabled us to quantify the extent of deformation at the mesoscale.

Importantly, ESEM is not the only microscopy technique that researchers have used to analyse the morphologic transformations of single particles of flexible MOFs. Gianneschi, Paesani *et al.*[31] employed environmental transmission electron microscopy (ETEM) to monitor, *in situ*, the flexible behaviour of MIL-53(Cr) individual crystals upon water sorption and upon temperature changes. They correlated their experimental results to computer simulations, which enabled them to precisely determine the structural changes induced by the water adsorption/desorption.

2.2. Transferring MOF flexibility to the macroscale: propagation

The concept of propagation in flexible MOF crystals can be clearly illustrated by the work reported by Kaskel *et al.*[1] In this research, the authors activated a defined quantity of flexible MIL-53(Al) ($[Al(OH)(bdc)]_n$; bdc = 1,4-benzenedicarboxylate) MOF powder, and then compacted it in a force-measuring bench equipped with both a force-transmission stamp and a height-measuring device. Next, they exposed the MOF sample to methanol or ethanol, which led to the expansion of the crystals and consequently, to the expansion of the compressed powder, which acted as a spring that pushed the stamp (Fig. 2a). Using this configuration, Kaskel and co-workers were able to measure the expansion forces and, by extension, evaluate the effects of the packing density on the mechanical response (Fig. 2b). They identified three different behaviours, according to the packing density. Thus, at low density, the voids between the crystals allowed them to expand freely, and the researchers only observed negligible forces. However, as the density increased, the voids decreased in size, thereby forcing the crystals to expand by pressing the stamp. In this domain, as the packing density increased, so did the registered expansion force. Finally, at the highest densities, the powder reached maximum compression, at which point it exhibited back-pressure to the stamp, generating detectable expansion force

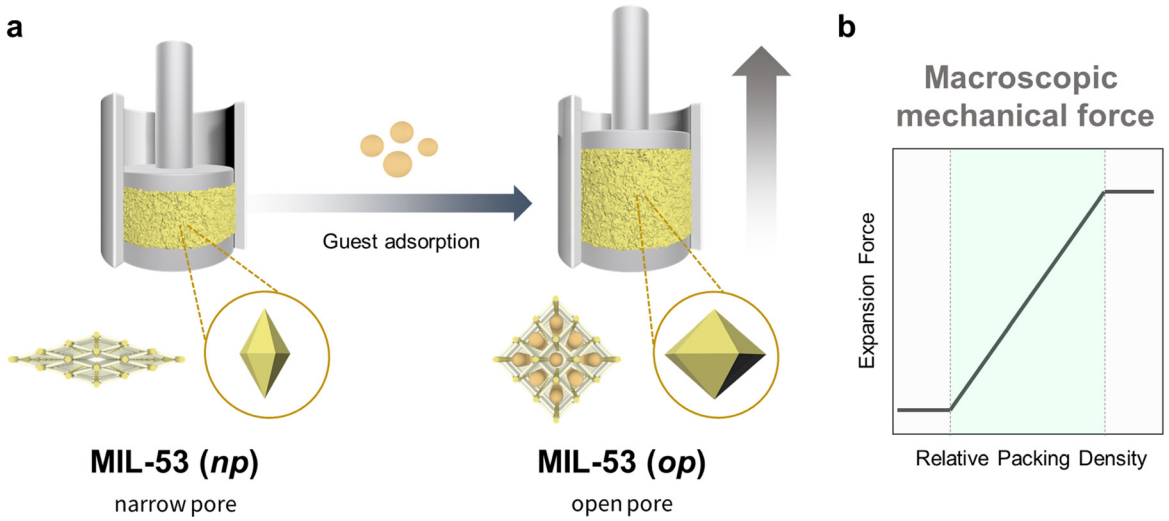

Fig. 2 Schematic of the experimental set-up for estimating the force exerted by compressed MIL-53(Al) powder upon adsorption (left), and a plot of the observed expansion force profile *vs.* MOF packing density (right).[1]

even before any solvent was added. Thus, Kaskel and colleagues not only demonstrated that variations in the crystal dimensions of MOFs could be transferred (and measured) at larger scales, but also evidenced that controlling the spatial distribution of MOF crystals is essential to attaining macroscopic responses.

Despite the obvious potential of flexible MOFs in mechanical actuation, their use as powders demands careful consideration for various reasons. Firstly, and as described above, to achieve a mechanical response at the macroscale, inter-crystal voids ideally should be removed to allow for the transmission of the individual crystal forces across the entire volume. This agglomeration can be done through direct compression of the MOF powder, resulting in a densely-packed bulk object. However, this processing method will still be limited by the resistance of the MOF to external mechanical stress, which can lead to structural collapse. Thus, this approach demands a compromise between the elimination of the inter-crystal voids and the loss of the initial MOF properties. Secondly, the use of pressed flexible MOF pellets involves the loss of their active form upon expansion, as crystal expansion will create new voids, thus requiring that the agglomeration step be repeated to enable further use. Finally, and contrary to what is observed for a single MOF crystal, whereby changes in unit-cell parameters involve deformations with preferential directions, the use of MOF powders, in which crystals are randomly distributed, implies the isotropic deformation of the formed object. Thus, one immediate consequence of moving from the mesoscale to the macroscale is a loss of directionally, which, as we discuss in the following section, implies certain design considerations.

3. Flexible MOF composites as actuators

In the previous section, we described how the structural transformations of flexible MOFs can be converted into useful work at the macroscale. However, the practical use of bare flexible MOF powders presents several limitations. In this sense, the fabrication of composites of flexible-MOFs and organic binders has proven fruitful for producing macroscopic objects with responsive behaviour. In this section, we cover recent progress in this area.

3.1 Flexible MOF crystals as responsive fillers

The limitations of using bare flexible MOF powders for mechanical actuation described in the previous section have motivated researchers to explore the incorporation of flexible MOF crystals, as responsive fillers, within a continuous matrix. This entails using a binder to eliminate the inter-crystal voids, to in turn allow for the transmission of mechanical forces. Moreover, the incorporation of the binder also confers the resultant composite with mechanical strength and cohesion. Obviously, the binder material must exhibit several characteristics that ensure operational functionality, which we outline below.

Firstly, the binder must be mechanically suitable to transfer the mechanical stress caused by the deformation of the MOF. Thus, it must be sufficiently flexible to be compressed by MOF crystals, which will lead to the propagation of the stress across the entire system, while being sufficiently elastic under working stress conditions, to enable a reversible response *via* expansion and contraction cycles. High compatibility between the MOF particles and the binder is critical to guarantee good contact, by reducing the presence of voids, as these would result in futile MOF deformation. The influence of the interaction between the binder and the MOF on its flexible behaviour has been evidenced by Zhao *et al.*, who used the flexible $[Cu(dhbc)_2(bpy)]_n$ (dhbc = 2,5-dihydroxybenzenedicarboxylate, bpy = 4,4′-bipyridine) MOF.[32] Intriguingly, after they had embedded this MOF into a polymeric (Pebax) matrix and heat-activated the resultant ensemble at 120 °C, the MOF retained its open-pore configuration; contrariwise, when they heat-activated the pristine bulk powder at 70 °C, it adopted the closed-pore configuration. Zhao and co-workers attributed this discrepancy to the

strong interactions between the Pebax polymer groups (*i.e.* –NH, –CO, –OH) and the free –OH groups at the surface of the MOF crystals.

Secondly, since most of the reported structural transformations of flexible MOFs are based on host–guest interactions, the binder material must allow for molecular transport throughout the entire MOF volume to enable MOF–adsorbate interactions. Great progress has been made in the design and fabrication of MOF-based, mixed-matrix membranes (MMMs), which now provide a foundation for developing efficient composite membranes capable of actuation.[33–36] For instance, methods for improving the MOF–polymer interaction, such as MOF surface functionalisation or pre-polymer coating, have been demonstrated to reduce the interfacial voids, thereby conferring the composite with better cohesion. Moreover, for conventional applications of MOF-based MMMs, such as separation, optimal performance of the membranes requires an even distribution of the crystals. However, as we mentioned before, such homogeneous distribution of the crystals is expected to provide an isotropic deformation, which is incompatible with mechanical actuation. Thus, conventional methods for fabricating MOF-based MMMs must be adapted to create composite membranes in which an inhomogeneous distribution of the MOF particles is achieved.

3.2 Asymmetric flexible-MOF films as mechanical actuators

The simplest way to create a mechanical actuator is probably to construct a bilayer comprising two materials with different

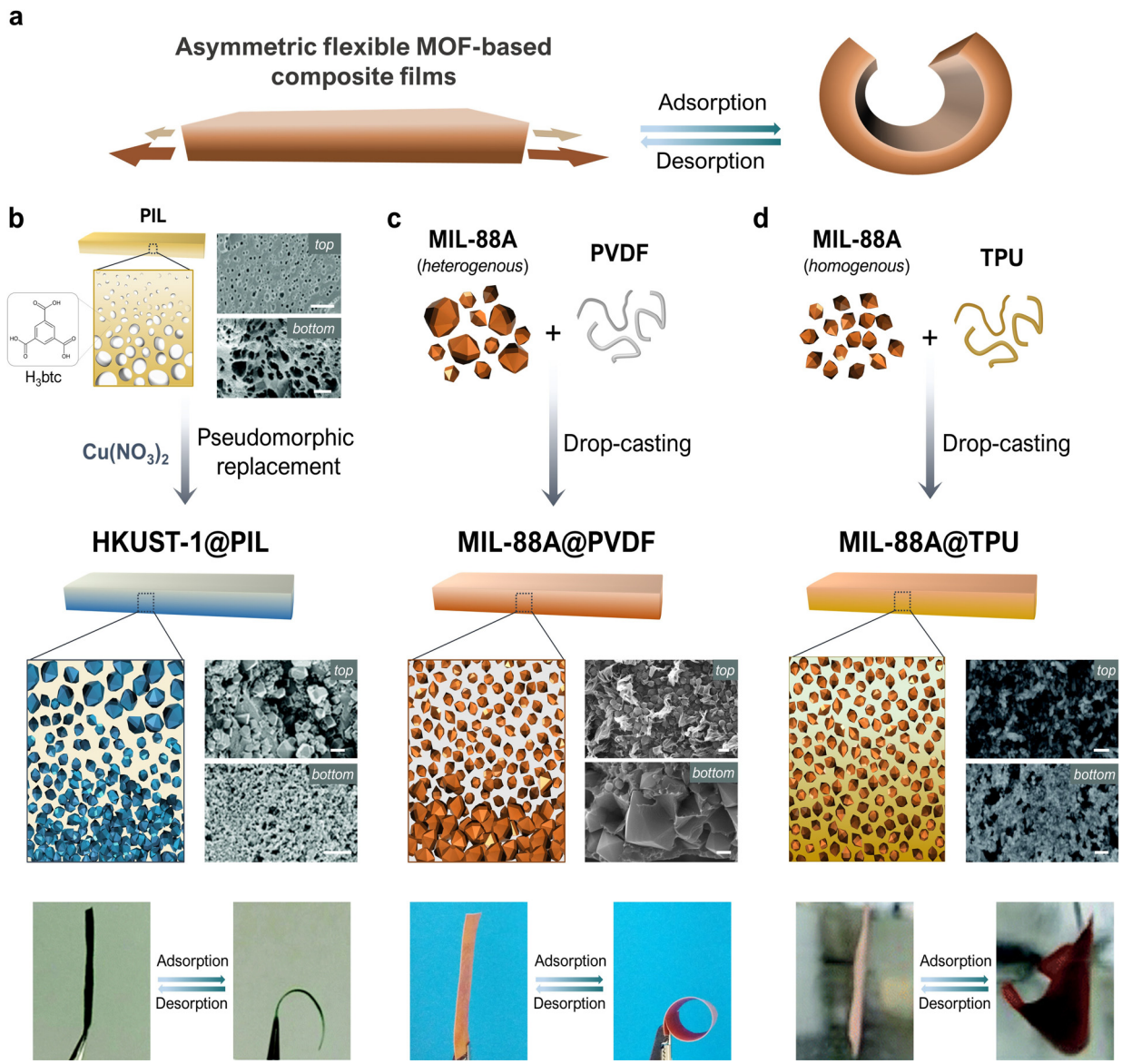

Fig. 3 Schematic of the folding mechanism in asymmetric, flexible-MOF, composite films (a). Schematic of the syntheses, and photographs illustrating the reversible bending, of asymmetric HKUST-1@PIL (b), MIL-88A@PVDF (c), MIL-88A@TPU (d) (scale bars = 2 μm). Adapted, with permission, from ref. 30, 38 and 40.

expansion coefficients that are bound together. In response to external stimuli, such an array undergoes swelling mismatch between the layers, which forces the entire structure to fold. Although this approach is simple, it can entail certain drawbacks, such as a lack of compatibility between the layers, or their potential separation due to the stress generated under working conditions.[37] These limitations have motivated researchers to develop single-layered systems, in which actuation is induced by asymmetric expansion across the thickness. Such asymmetry can be achieved by various means, such as by generating different levels of crosslinking, localizing distinct crystalline phases, or creating a compositional gradient *via* embedding of extrinsic fillers. Correspondingly, MMMs can be designed to present a vertical flexible-MOF gradient, such that the greater swelling of the MOF-rich side will cause the membrane to fold (Fig. 3a).

This concept was first demonstrated by Yuan *et al.*, who reported the fabrication of an asymmetric composite film constructed from HKUST-1 ($[Cu_3(btc)_2]_n$; btc = 1,3,5-benzenetricarboxylate) and poly(ionic liquid) (PIL) polymer, *via* coordination-driven pseudomorphic replacement.[38] First, they formed an asymmetric PIL film with an ionic cross-linking gradient, in which they employed H_3btc/btc^{3-} linker as anionic component. Next, they replicated the asymmetric structure by immersing the film into a $Cu(NO_3)_2$ solution, which led to the formation of HKUST-1 crystals. Thus, the asymmetric structure of the initial polymeric film was maintained, yielding the asymmetric composite film, HKUST-1@PIL, which contained a higher concentration of HKUST-1 crystals at one side (Fig. 3b). This asymmetry conferred the film with actuation capacity in response to NH_3 vapor, which the authors attributed to the expansion of HKUST-1 crystal volume upon adsorption of NH_3. Additionally, Yuan and colleagues were able to recover the original shape of the membrane by heating the film; however, after a few adsorption/desorption cycles, they observed a decrease in the curvature, which they attributed to the high affinity of NH_3 gas for HKUST-1. Their report clearly evidenced the capacity of flexible MOFs to form asymmetric structures capable of folding in response to chemical stimuli. However, the mechanical response of HKUST-1 crystals upon adsorption is modest, and implies only very slight structural deformations.[39] Moreover, the *in situ* formation of the MOF inside the membrane imposes more limitations on control over the crucial aspects of the crystals, such as their size, shape, and defects, and demands that the conditions used for MOF synthesis be compatible with the pre-formed asymmetric membrane. Reflecting on the above limitations, our group conceived of a more-general strategy to produce asymmetric composite films, based on drop-casting, a method that had already been widely used for preparing MOF-based MMMs,[35,36] due to its simplicity and versatility. Briefly, pre-formed MOF crystals are dispersed into an organic polymer solution, the resultant dispersion is deposited into a substrate, and the solvent is evaporated off to yield a composite film. Typically, such MOF-based MMMs are intended for separation applications, for which a homogenous MOF dispersion is crucial for optimal performance. Therefore, control over both the size and the monodispersity of the MOF particles is critical to ensure high dispersibility of the crystals as well as optimal homogeneity of the resultant membrane.

Consequently, thinking in the opposite direction, using MOFs with a broad size distribution could provide the level of heterogeneity needed for actuation. To illustrate this principle, our group produced asymmetric composite films by combining pre-synthesised MIL-88A ($[Fe_3OH(X)_2(fumarate)_3]_n$; X = Cl, OH) MOF crystals having a broad size distribution (0.5 μm to 9.0 μm), with PVDF (polyvinylidene difluoride) as polymeric binder. This heterogeneity that we achieved resulted in differential sedimentation during solvent evaporation, causing the larger crystals to accumulate at the bottom, which in turn generated a vertical gradient of MOF-crystal distribution across the thickness (Fig. 3c). We chose MIL-88A owing to its well-known swelling behaviour, which involves the gradual enlargement of the MOF unit cell caused by the changes in pore-size during adsorption/desorption. Additionally, and as we mentioned in Section 2.1, the swelling behaviour of a single crystal of MIL-88A had previously been studied by ESEM, and its structural transformation was found to be guest-selective: when the MOF crystals were exposed to non-polar molecules, no response was observed. Moreover, the shape, size, and size dispersity of MIL-88A crystals can be precision-tuned by changing the synthetic conditions. Besides, PVDF exhibits several features, such as high chemical stability and excellent mechanical properties, which have been exploited to produce various MOF-based MMMs.

As we had expected from its asymmetric structure, our MIL-88A@PVDF film exhibited reversible self-folding upon immersion in water and different organic solvents. To confirm that the driving force responsible for such behaviour was indeed the reversible expansion/contraction of MIL-88A crystals, we fabricated and subsequently tested bare polymeric film, and non-flexible MOF (MIL-100, $[Fe_3O(OH)(btc)_2]_n$; and MOF-801, $[Zr_6O_4(OH)_4(fumarate)_6]_n$) composite films with asymmetrically distributed MOF crystals. Importantly, none of them showed any response. Furthermore, we observed that the solvents that did (or did not) induce folding of the films were the same ones that did (or did not) cause swelling of MIL-88A crystals, which corroborated that MOF crystals were indeed the component behind the actuation.

Having ascertained the role of the MOF in the folding response, we next studied the relationship between the MOF and macroscopic phenomena that we had observed, by tracking the changes in its water-vapour uptake, XRPD spectra, and folding response, upon increasing (adsorption) and then decreasing (desorption) the levels of relative humidity (RH) (Fig. 4). These experiments revealed how the adsorption profile of the MOF corresponds to structural transformations of the crystals, which simultaneously correspond to the macroscopic deformation of the films. As the RH gradually increased (up to 90%), so did the folding response. Interestingly, when the RH decreased, the films did not begin to unfold until *ca.* 40% RH. This observed shape-memory effect can be explained by the hysteresis on the respective water-sorption isotherms for bare MIL-88A crystals and for MIL-88A@PVDF films. Thus, due to the high affinity of the MOF network for water, desorption at

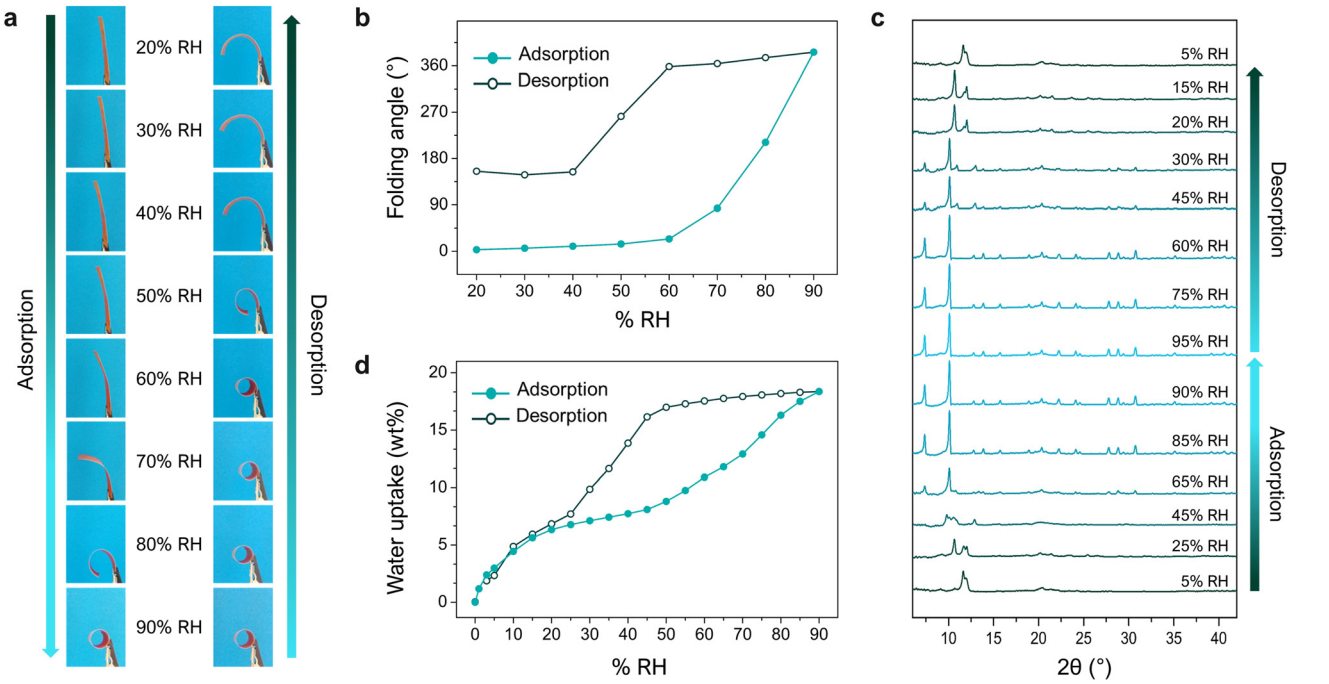

Fig. 4 (a) Photographs of an asymmetric MIL-88A@PVDF film after 15 min under different levels of relative humidity (RH): from 20% up to 90% (adsorption), and from 90% back down to 20% (desorption). (b) Plots of changes in the folding-angle of MIL-88A@PVDF films in function of RH, from 20% to 90% (adsorption; solid dots) and then decreasing back to 20% (desorption; outlined dots). (c) *In situ* XRPD of a MIL-88A@PVDF film undergoing adsorption and desorption of water-vapour. (d) Water-vapour adsorption isotherm for an asymmetric MIL-88A@PVDF film at 25 °C (solid dots: adsorption; outlined dots: desorption). Adapted, with permission, from ref. 30.

room temperature is less favoured at medium-high RH levels, resulting in a lack of mechanical response (shrinkage). Briefly, the mismatch between the adsorption and desorption branches of the MOF isotherm (*i.e.* hysteresis) translates into an equivalent mismatch between adsorption and desorption folding-response (*i.e.* shape-memory). This work offered a simple, adaptable, and efficient strategy to construct actuators by exploiting the flexibility of MOFs. In principle, this method enables the incorporation of any flexible MOF into a polymeric matrix, whereby the control over the size and dispersity of the MOF crystals is crucial for accessing self-folding capabilities. Furthermore, the response of asymmetric flexible-MOF composite films is determined by the MOF-crystal deformations, which in turn depend on the specific type of host–guest interactions. This scenario makes the design of actuators with specific features possible through the rational selection of flexible MOFs.

The versatility of the concept described above has been further demonstrated by Zheng *et al.*, who prepared an asymmetric, flexible-MOF composite film, similar to MIL-88A@PVDF, but instead based on the MOF MIL-88C ($[Fe_3OH(X)_2$(2,6-naphthalene dicarboxylate)$_3]_n$; X = Cl, OH).[40] MIL-88C MOF is isoreticular to MIL-88A, exhibiting larger, more-hydrophobic pores, due to the naphthalene-based linker. Thus, the resulting responsive asymmetric MIL-88C@P(VDF-CTFE) (PCTFE = polychlorotrifluoroethylene) film not only functioned as an actuator, but also exhibited the same guest-response selectivity as bare MIL-88C crystals do. Therefore, whilst MIL-88A@PVDF films exhibited actuation when exposed to water or polar organic solvents, they did respond to less-polar solvents. Interestingly, the MIL-88C@P(VDF-CTFE) films exhibited the opposite behaviour: they did not respond to water, but did bend when treated with toluene or dichloromethane.

Yet another method for the preparation of MIL-88 MOF composite films has been conceived of by Guo *et al.*,[41] who employed a different polymeric matrix to produce MIL-88A@TPU (TPU = thermoplastic polyurethane) composite films. Firstly, they prepared MIL-88A crystals with a more narrow size distribution, by following a surfactant-assisted method.[42] Then, they studied the effects of increasing the MOF-loading, by preparing composite films in which the MIL-88A crystals were homogeneously distributed. Despite this symmetric MOF arrangement, the resulting films still folded in response to water. Guo and co-workers attributed this behaviour to the vertical-gradient distribution of the TPU phase, which was located mainly at the bottom layer (Fig. 3d). Thus, in this denser region, MIL-88A crystals could transfer the mechanical stress to the surrounding medium more effectively, thus causing the film to fold towards the upper part. This example of film actuation operates by a mechanism distinct from that of the previously cited examples of MIL-88A@PVDF and MIL-88C@P(VDF-CTFE). Nonetheless, in all three cases, the guiding principle remains the strategic use of vertical gradients, such that swelling of the flexible MOF triggers a mechanical response.

The examples that we have described in this section not only evidence that MOF-crystal deformations can be exploited for mechanical actuation, but they also illustrate how the behaviour of the resultant responsive films could be controlled.

Thus, the nature of the flexible MOF structural transformation, the size and dispersion of the crystals, and the polymer used as a binder will each influence the response. However, an important limitation of the first-generation films described here is that they only exhibit vertical gradients; as such, their actuation capacities are limited to uniaxial deformations, thus narrowing their potential applications. Accordingly, the next advance for researchers was to engineer new MOF-based composite films capable of performing more-complex 2D-to-3D shape transformations.

3.3 Controlling the spatial distribution of flexible MOF crystals: patterning

Smart films that could undergo predictable, reversible, 2D-to-3D shape-transformations would have countless applications in soft robotics,[43–46] (bio)sensing,[47–49] biomedicine,[50,51] and engineering,[52] among other fields. However, as we previously mentioned, the construction of flexible-MOF composite films that contain only vertical gradients limits access to more-complex 3D structures. To achieve such 3D self-shaping, the actuator must present multi-axial deformation, which means that MOF composite films must exhibit both vertical and lateral heterogeneity. Therefore, programmable 2D-to-3D shape transformations would demand having control over the spatial distribution of the responsive MOF filler over the entire film. To date, this challenge has been addressed by following multi-step methods, due to the difficulty in precisely localising MOF particles within the polymeric matrix during its formation.

The first example of a programmable, 3D, self-shaping, MOF-based film was developed by our group.[53] Our strategy involves the controlled chemical etching of non-responsive homogenous MIL-88A@PVDF films, which enables the creation of MOF-containing and MOF-free domains by patterning (Fig. 5). We initially employed the surfactant-assisted method[42] to produce smaller, more monodisperse MIL-88A crystals than those obtained with other methods, and then combined these crystals with PVDF to generate homogenous MIL-88A@PVDF composite films. As we had expected, these films did not function as actuators, due to their lack of directionality. Next, following our controlled-etching strategy, we exposed one side of the film to HCl gas at room temperature for a period of time (Fig. 5a). These experiments yielded responsive asymmetric composite films in which the MIL-88A crystals located at the exposed side were removed, while the rest remained untouched. As the exposure time increases, so does the volume of HCl that diffuses into the composite film, and consequently, the amount of MOF that is etched; thus, the degree of etching can be controlled by selective use of exposure time. Remarkably, the different ratios between the MOF and the non-MOF domains leads to distinct types of bending. Thus, as the vertical etching increased, so did the self-folding capacity, until eventually reaching a performance maximum; in fact, any further increases in etching actually led to a reduction in folding response. We rationalised this observation by considering the balance between two antagonistic effects of the etching: on one hand, the creation of an asymmetric

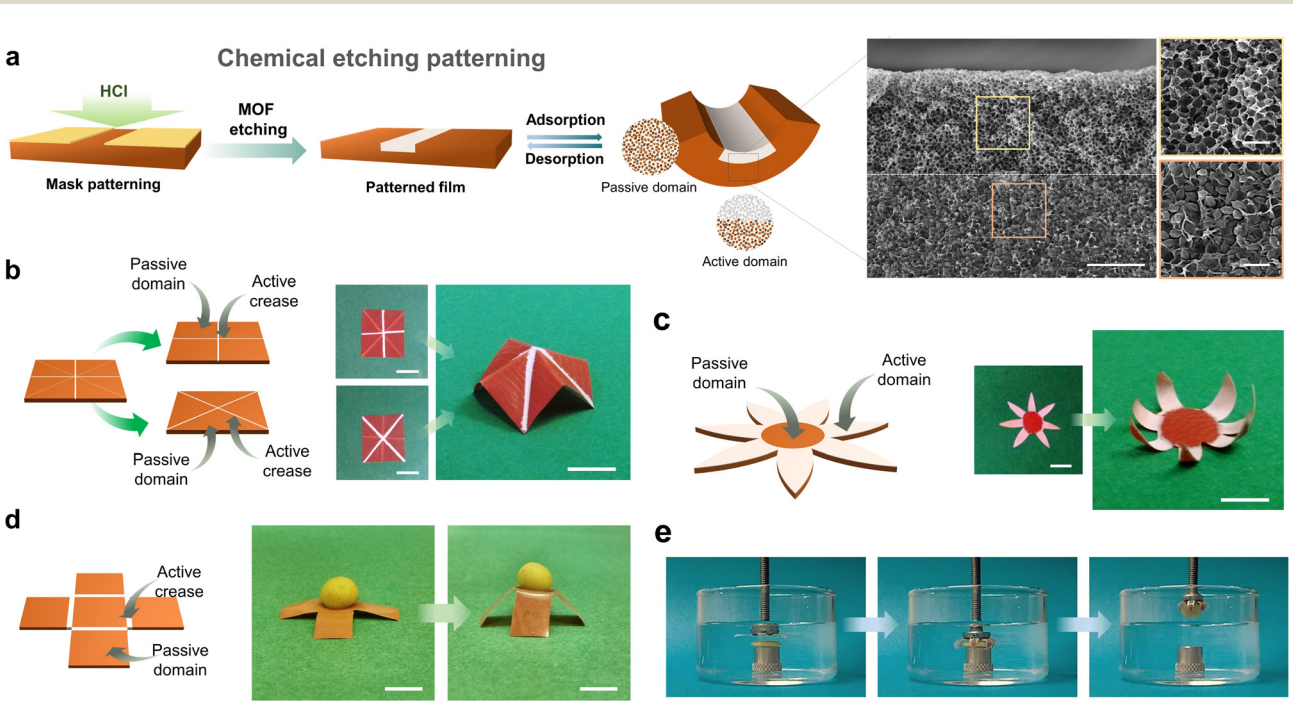

Fig. 5 (a) Schematic representation of the patterning of MIL-88A@PVDF films by chemical etching with HCl. (b) Schematic of four-pointed star patterned MIL-88A@PVDF structure (left) and photographs of its 2D to 3D shape transformation upon exposure at 90% RH (right). Scale bars = 1 cm. (c) Schematic of seven-petal flower patterned MIL-88A@PVDF structure (left) and photographs of its 2D to 3D shape transformation upon exposure at 90% RH (right). Scale bars = 5 mm. (d) Schematic of open cube patterned MIL-88A@PVDF structure (left) and photographs of its 2D to 3D shape transformation, lifting cargo that is five-times heavier upon exposure at 90% (right). Scale bars = 5 mm. (e) Self-folding claw application of patterned MIL-88A@PVDF seven-petal flower structure, gripping a modelling-clay disc immersed in warm water. Adapted, with permission, from ref. 53.

structure, which favours actuation; and on the other hand, the removal of active fillers, which disfavours actuation.

Having demonstrated the efficiency of this method for generating controlled vertical gradients, our next step was to create lateral gradients. To this end, we developed a mask-patterning method by attaching an adhesive Kapton tape mask to the film surface, and then further treating the film with HCl. This procedure enabled us to create active domains (*i.e.* the exposed areas), in which the removal of MOF crystals induced folding by generating hinges, and passive domains (*i.e.* the unexposed areas), which did not exhibit any folding response. The demonstration of these predictable 2D-to-3D shapeshifts opened a whole range of possibilities for fabricating complex 3D structures with well-defined functionalities inspired by origami and kirigami designs. Thus, by following the same patterning strategy, we were able to design and fabricate a set of various programmable self-shaping films that executed different mechanical tasks such as lifting, grabbing, and walking.

First, we demonstrated controllable 2D-to-3D self-shaping for MIL-88A@PVDF by fabricating a patterned film capable of reversibly assembling into a 3D four-pointed star (Fig. 5b). To this end, we patterned two plus-signs, oriented at 45° to each other, at both sides of a square film (*i.e.* one plus-sign per side), which enabled upwards and downwards folding. Next, we prepared a seven-petal flower, based on active (etched) petals that fold towards a passive (non-etched) centre, in what we called reverse-blooming. We then extended this process to the mechanical task of grabbing: by exposing the seven-petal flower to water, it worked a mechanical claw, gripping a modelling-clay disc 15-times heavier than itself (Fig. 5e). We further demonstrated the working capacity of MIL-88A@PVDF films by fabricating an open-cube structure capable of lifting cargo 20-times its own weight (Fig. 5d). Another mechanical function that we explored with flexible-MOF composite films was unidirectional walking. Thus, we prepared a worm-like crawling actuator comprising an active domain (etched; 60% of the total length) and a passive domain (non-etched; 40% of the total length) with a fully etched region. We exposed the film to alternating UV/Vis irradiation cycles under constant relative humidity, which led to differential responses across the film length, thereby resulting in unidirectional motion.

Researchers have explored other, non-etching based patterning techniques to confer MOF composite films with mechanical functions. For instance, Guo *et al.*[41] devised template patterning and laser-ablation patterning. In the former, they casted a solution of MOF (MIL-88C) crystals and P(VDF-CTFE) polymer onto a microchannel-patterned PDMS (polydimethylsiloxane) template, and then dried it to obtain a film with microchannels. In the latter method, they applied femtosecond laser radiation to a pre-formed MIL-88C@P(VDF-CTFE) film, creating micro-structured patterns with precise control over the pattern width and depth. Next, Guo and co-workers demonstrated that each of their two methods could be used to pattern films that could undergo programmable and reversible 2D-to-3D shapeshifting. Thus, similarly to our work with self-shaping MIL-88A@PVDF films, they fabricated a six-petal gripping-flower and a unidirectional walking device, both of which actuated in response to dichloromethane.

3.4 Alternative designs

Two-dimensional films are not the only functional composites that have been generated by exploiting MOF flexibility.

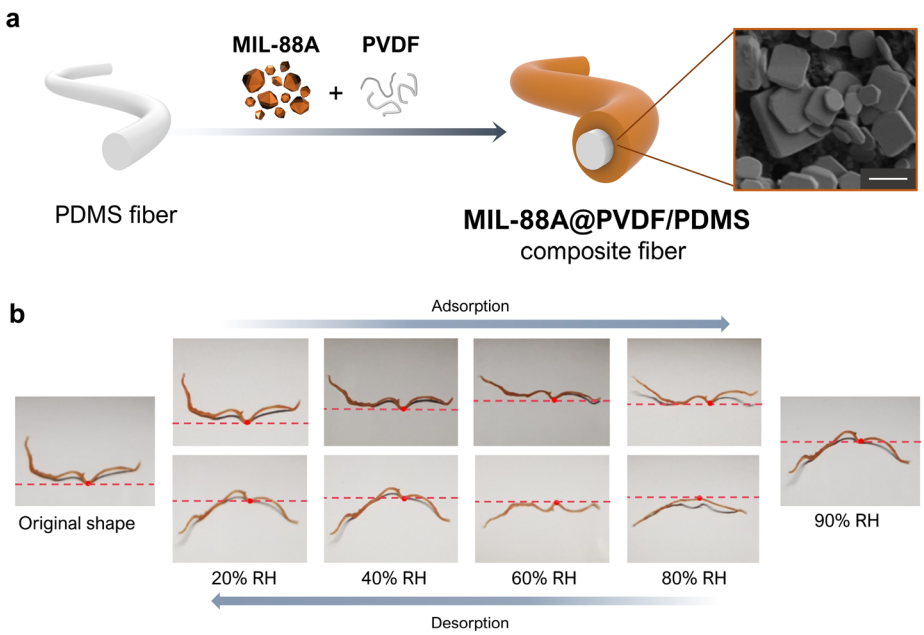

Fig. 6 (a) Schematic of the fabrication of the MIL-88A@PVDF/PDMS fibres (left). SEM image of a MIL-88A@PVDF/PDMS fibre, revealing the embedding of MIL-88A within the PVDF polymer matrix (right). Scale bar (1 μm). (b) Photographs of the deformation of MIL-88A@PVDF/PDMS fibre upon exposure to different levels of relative humidity (RH): from 20% up to 90% (adsorption), and from 90% back down to 20% (desorption). Adapted, with permission, from ref. 54.

For example, Wan *et al.* fabricated a humidity-sensitive fibrous composite, MIL-88A@PVDF/PDMS, in which they supported a MIL-88A@PVDF layer onto a core PDMS fibre (Fig. 6a).[54] To prepare the composite fibres, they first produced PDMS fibres by wet-spinning. Next, they evenly drop-coated a DMF solution of MIL-88A crystals, which were very heterogeneous in size, and PVDF onto the obtained PDMS fibre. After drying, the analysis of the resulting composite fibre revealed that the MOF crystals had distributed broadly across the external PVDF layer. Although these MIL-88A@PVDF/PDMS composites could be considered to be analogous to the aforementioned MIL-88A@PVDF films, their 1D fibrous structure, as well as their swellable polymeric core, together created a distinct actuation response. The clearest difference between the two materials is that deformation in the 1D fibrous actuators is less restricted than in 2D films, since fibres can undergo axial extension and twisting, radial expansion, bending, or some combination thereof.[55] Otherwise, the responsiveness of MIL-88A@PVDF/PDMS upon water sorption is analogous to that of MIL-88A@PVDF films. Thus, when exposed to increasing humidity levels from 10% to 90% RH, the fibres gradually stretched according to the swelling properties of MIL-88A. Correspondingly, when RH was reduced from 90% to 10% RH, the fibres shrank, due to the desorption of water by the MIL-88A crystals and their consequent shrinkage (Fig. 6b). However, this shrinking process upon desorption did not allow the fibres to return to their initial state. Thus, the responsive behaviour of MIL-88A@PVDF/PDMS fibres is analogous to that observed for MIL-88A@PVDF films, in which a similar shape-memory effect was described (see above). Finally, Wan *et al.* also investigated the response of their composite fibres to immersion in different organic solvents, registering three different solvent-dependent responses. As expected, when they soaked the fibres in polar solvents (*e.g.* water, ethanol, or acetonitrile), the fibres stretched, due to the high affinity of MIL-88A crystals for these solvents. However, when they soaked the fibres in non-polar solvents (*e.g.* toluene and trichloromethane), which cannot induce shapeshifting of MIL-88A, the fibres underwent irregular changes in shape. The authors attributed this phenomenon to the swelling of the inner hydrophobic PDMS core, which exhibits greater affinity for those solvents. Finally, when soaked in acetone, the fibres initially bent and subsequently stretched. This dual response stemmed from the combined swelling of initial (external) MIL-88A crystals and subsequent (internal) PDMS layers. Wan and colleagues further corroborated the role of PDMS on the observed responses of their MIL-88A@PVDF/PDMS fibres, using tensile stress–tensile strain measurements. Interestingly, whereas the fibres soaked in acetone, toluene, or trichloromethane suffered a marked deterioration in their mechanical properties, those soaked in ethanol or water exhibited minimal or negligible damage, respectively.

The aforementioned work by Wan and co-workers clearly illustrated that the incorporation of an additional component into flexible-MOF composites could confer them with added functionalities and thus, broader perspectives for applications. Accordingly, researchers have developed materials that, in addition to mechanical actuation, exhibit complementary responsive behaviour. For example, Jia *et al.* reported a dual-response, MIL-88A/CB@PVDF (where CB = carbon black) composite-film actuator (Fig. 7a).[56] Here, in addition to achieving a folding response through asymmetric distribution of MIL-88A crystals, the authors also generated a reverse opal structure to provide the film with photonic properties. To this end, they drop-casted a solution of MIL-88A, CB and PVDF onto a SiO_2 photonic crystal template, and then heated it to remove the solvent. Next, they exposed the side containing the SiO_2 template to HF vapour to induce chemical etching. This process simultaneously yielded two outcomes: (i) the formation of a

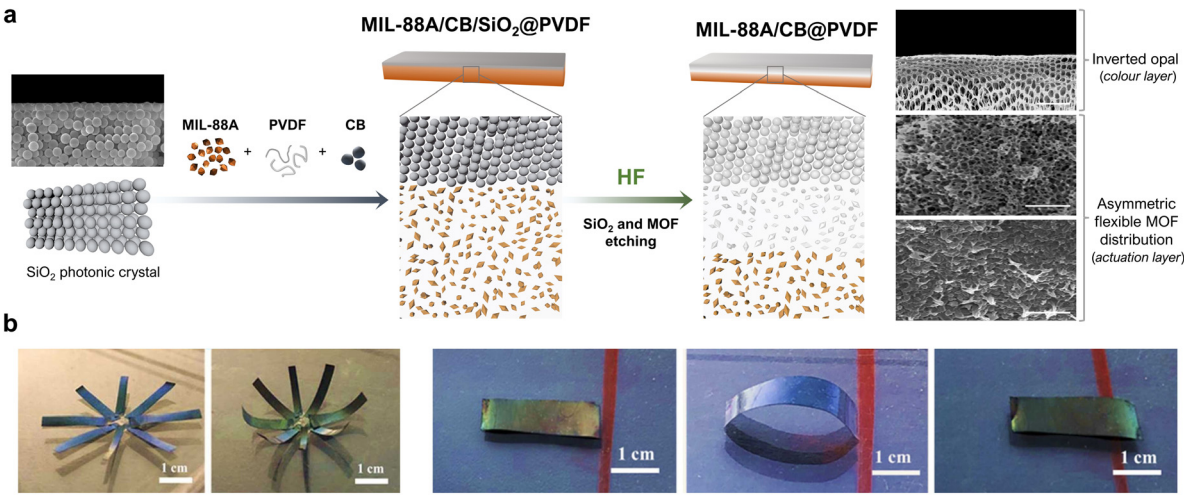

Fig. 7 (a) Schematic of the fabrication of the MIL-88A/CB@PVDF, inverted-opal, dual-response film. (b) SEM image of a cross-section of a MIL-88A/CB@PVDF reverse-opal film, showing the inverted-opal structure (top of film); the region where the MIL-88A was partially etched (middle of film); and the intact structure of MIL-88A/CB@PVDF (bottom of film). (c) Photographs of a MIL-88A/CB@PVDF eight-petal flower, which blooms in a methanol atmosphere. (d) Photographs of a dual-response, MIL-88A/CB@PVDF, worm-like crawling actuator in a methanol atmosphere. Adapted, with permission, from ref. 56.

reverse opal structure, due to the removal of the SiO_2 template, and (ii) the asymmetric distribution of MIL-88A crystals across the film thickness. The morphological analysis of these films revealed three consecutive layers: a reverse opal layer; an etched-MOF layer; and a non-etched-MOF layer. The etched MIL-88A/CB@PVDF films exhibited excellent actuation performance, analogous to that of the aforementioned MIL-88A@PVDF films, owing to their similar asymmetric structures. Moreover, the reverse-opal PVDF photonic structure conferred the resultant film with the ability to change colour under different viewing angles. Wan and co-workers then demonstrated that these two properties could be combined to develop a dual-response methanol-vapour sensor. The principle of this device lies in the dependence of the film curvature on the methanol concentration, as well as the change in the film colour due to the change in the curvature. Thus, as the methanol concentration increases, the film bends further and consequently, the colour observed by the naked eye shifts further red to enable detection of the vapour.

4. Conclusions and outlook

The conversion of the swelling or shrinking of a chemically responsive material into mechanical work makes it possible to exploit environmental changes for transmitting and/or harvesting energy. Researchers have broadly investigated this concept in the field of soft robotics, in which flexible materials are designed to execute controlled autonomous motion in response to external stimuli. Flexible MOFs offer an alternative platform compared to purely organic or inorganic materials, not only due to their outstanding porosity, but also because of the synthetic control now possible for their composition, pore structure, chemical functionalisation, and crystal morphology and size. In addition, their crystalline nature makes it possible to track the structural changes with high precision by using X-ray diffraction techniques. Flexible MOFs have recently made their foray into soft robotics, demonstrating their potential use in smart devices and systems capable of executing autonomous tasks. The pioneering work in this area indicates that the responsive behaviour arising from MOF–guest interactions can be transferred across multiple length scales and that the macroscopic response can be predicted by understanding structure–property relationships. This latter aspect is quite advantageous, since MOF crystalline porous frameworks can be designed to present myriad characteristics by reticular chemistry and tuned by post-synthetic modification. For instance, asymmetric composite films of isoreticular MIL-88A or MIL-88C respond differently to polar and non-polar guest molecules, due to their distinct respective linkers.

The field of MOF-based actuators remains embryonic: indeed, the number of responsive devices based on flexible MOFs is still limited. The devices that we have cited in this review had been constructed as asymmetric films or, to a lesser extent, 1D composite fibres or 3D bulk-powders. Most of these first-generation devices were intended merely for proof-of-principle or as prototypes. Thus, the establishment of comparative parameters to enable systematic analysis of multiple device parameters (*e.g.* MOF type, linker type, MOF-loading, curvature, thickness, *etc.*), the assessment of long-term stability, as well as performance reproducibility, will be invaluable for further advances.

We recognise that the functionalities of flexible-MOF actuators are not yet as sophisticated as those of other systems. A major challenge for researchers is to achieve control over the spatial location of responsive particles within a fabricated device. Two main approaches to create asymmetric porous materials at the macroscale are of interest here: single-step fabrication, in which all the steps occur simultaneously; and stepwise fabrication, in which the device is built sequentially.[57] Likewise, reported strategies for positioning of MOF particles,[58] such as pseudomorphic replication,[59] electrodeposition,[60] and magnetic alignment,[61] should be revisited. Here, the enormous knowledge gained from decades of MOF research offers a solid foundation on which to gain greater control and access a wider design catalogue. In this context, we strongly believe that interdisciplinary, especially among experts in Materials Science, Organic & Inorganic Chemistry, and Physical & Chemical Simulations, will be cardinal to success.

Although this line of research is in its infancy, several recent publications point to future directions.[62,63] Various groups have demonstrated that the highly porous and ordered structures of MOFs are suitable to develop systems whose response to external stimuli yields mechanical motion. Such autonomous MOF-based motors rely on different mechanisms. For example, Matsui *et al.* reported a device in which the partial decomposition of a MOF, and subsequent release of loaded peptide molecules, triggered autonomous swimming motion, *via* the Marangoni effect.[64] Similarly, our group has engineered different types of self-propelled MOF particles: metallic Janus MOF particles with a catalytic Pt coating;[65] and hierarchical micro/mesoporous structures loaded with an active enzyme.[66] An important consideration is that MOFs can exhibit diverse physical/chemical properties that could be exploited to achieve work. For instance, Wang, Xu *et al.* recently prepared near-infrared (NIR) light-driven, hydrogel actuators, by using MOF particles as photothermal nanotransducers.[67] Likewise, Wang *et al.* reported that flexible MOFs could be combined with other materials to generate 1D photonic crystals, in which MOF deformations provoke an optical response.[68]

Overall, we believe that the applications of such MOF-based devices can range from highly sensitive/selective chemical detectors and controlled delivery systems, thanks to their high microporosity with precise pore design, to soft grippers, artificial muscles, or flexible triboelectric generators. In addition, the field of porous-material actuators could be further advanced by encompassing other reticular porous materials, such as covalent-organic frameworks (COFs) and molecular metal organic polyhedra (MOPs), which could be regarded as the purely organic or purely molecular analogues of MOFs, respectively. In fact, recent examples illustrate that such materials can indeed be used for creating mechanically responsive systems. For instance, Yan *et al.* hybridised MOPs with polymers, thereby

creating a gradual change in MOP crosslinking across the film thickness, to create soft actuators.[69] As for COFs, Zhang *et al.* has introduced gas-responsive groups into the COF structure to obtain a new series of responsive materials.[70] Interestingly, by incorporating flexible polymer chains into the COF structure, the same group was able to fabricate flexible COF-based membranes with vapor-responsive performance.[71] These purely organic materials possess excellent chemical and mechanical stabilities, and therefore, should be promising expansions to the preliminary arsenal of flexible-MOF actuators. Regardless, we are confident that the future is bright for shapeshifting materials based on actuators assembled from flexible-MOF composites and similar materials.

Conflicts of interest

There are no conflicts to declare.

Acknowledgements

This work was supported by the Spanish MINECO (project RTI2018-095622-B-I00) and the Catalan AGAUR (project 2017 SGR 238). It was also funded by the CERCA Pro-gram/Generalitat de Catalunya. ICN2 is supported by the Severo Ochoa program from the Spanish MINECO (Grant No. SEV-2017-0706). J. T. is grateful to the Spanish Ministry of Universities and the European Union through the Funds Next Generation through grant Maria Zambrano-UAM.

Notes and references

1 P. Freund, I. Senkovska, B. Zheng, V. Bon, B. Krause, G. Maurin and S. Kaskel, *Chem. Commun.*, 2020, **56**, 7411–7414.
2 S. Kitagawa and M. Kondo, *Bull. Chem. Soc. Jpn.*, 1998, **71**, 1739–1753.
3 C. Serre, F. Millange, C. Thouvenot, M. Noguès, G. Marsolier, D. Louër and G. Férey, *J. Am. Chem. Soc.*, 2002, **124**, 13519–13526.
4 R. Kitaura, K. Seki, G. Akiyama and S. Kitagawa, *Angew. Chem., Int. Ed.*, 2003, **42**, 428–431.
5 S. Horike, S. Shimomura and S. Kitagawa, *Nat. Chem.*, 2009, **1**, 695–704.
6 A. Schneemann, V. Bon, I. Schwedler, I. Senkovska, S. Kaskel and R. A. Fischer, *Chem. Soc. Rev.*, 2014, **43**, 6062–6096.
7 G. Férey and C. Serre, *Chem. Soc. Rev.*, 2009, **38**, 1380–1399.
8 F. Millange, C. Serre and G. Férey, *Chem. Commun.*, 2002, 822–823.
9 A. Modrow, D. Zargarani, R. Herges and N. Stock, *Dalton Trans.*, 2011, **40**, 4217–4222.
10 N. Yanai, T. Uemura, M. Inoue, R. Matsuda, T. Fukushima, M. Tsujimoto, S. Isoda and S. Kitagawa, *J. Am. Chem. Soc.*, 2012, **134**, 4501–4504.
11 R. Lyndon, K. Konstas, B. P. Ladewig, P. D. Southon, P. C. J. Kepert and M. R. Hill, *Angew. Chem., Int. Ed.*, 2013, **52**, 3695–3698.
12 W. Chapman, G. J. Halder and P. J. Chupas, *J. Am. Chem. Soc.*, 2009, **131**, 17546–17547.
13 S. A. Moggach, T. D. Bennett and A. K. Cheetham, *Angew. Chem., Int. Ed.*, 2009, **48**, 7087–7089.
14 Y. Wu, A. Kobayashi, G. J. Halder, V. K. Peterson, K. W. Chapman, N. Lock, P. D. Southon and C. J. Kepert, *Angew. Chem., Int. Ed.*, 2008, **47**, 8929–8932.
15 S. Krause, V. Bon, I. Senkovska, U. Stoeck, D. Wallacher, D. M. Többens, S. Zander, R. S. Pillai, G. Maurin, F.-X. Coudert and S. Kaskel, *Nature*, 2016, **532**, 348–352.
16 W. Li, M. R. Probert, M. Kosa, T. D. Bennett, A. Thirumurugan, R. P. Burwood, M. Parinello, J. A. K. Howard and A. K. Cheetham, *J. Am. Chem. Soc.*, 2012, **134**, 11940–11943.
17 Y. Sakata, S. Furukawa, M. Kondo, K. Hirai, N. Horike, Y. Takashima, H. Uehara, N. Louvain, M. Meilikhov, T. Tsuruoka, S. Isoda, W. Kosaka, O. Sakata and S. Kitagawa, *Science*, 2013, **339**, 193–196.
18 L. Sarkisov, R. L. Martin, M. Haranczyk and B. Smit, *J. Am. Chem. Soc.*, 2014, **136**, 2228–2231.
19 J. D. Evans, V. Bon, I. Senkovska, H.-C. Lee and S. Kaskel, *Nat. Commun.*, 2020, **11**, 2690.
20 S. M. J. Rogge, M. Waroquier and V. Van Speybroeck, *Nat. Commun.*, 2019, **10**, 4842.
21 F.-X. Coudert, M. Jeffroy, A. H. Fuchs, A. Boutin and C. Mellot-Draznieks, *J. Am. Chem. Soc.*, 2008, **130**, 14294–14302.
22 N. Behera, J. Duan, W. Jin and S. Kitagawa, *EnergyChem.*, 2021, **3**, 100067.
23 H. Sato, W. Kosaka, R. Matsuda, A. Hori, Y. Hijikata, R. V. Belosludov, S. Sakaki, M. Takata and S. Kitagawa, *Science*, 2014, **343**, 167–170.
24 N. Yanai, K. Kitayama, Y. Hijikata, H. Sato, R. Matsuda, Y. Kubota, M. Takata, M. Mizuno, T. Uemura and S. Kitagawa, *Nat. Mater.*, 2011, **10**, 787–793.
25 P. Horcajada, T. Chalati, C. Serre, B. Gillet, C. Sebrie, T. Baati, J. F. Eubank, D. Heurtaux, P. Clayette, C. Kreuz, J.-S. Chang, Y. K. Hwang, V. Marsaud, P.-N. Bories, L. Cynober, S. Gil, G. Férey, P. Couvreur and R. Gref, *Nat. Mater.*, 2010, **9**, 172–178.
26 L. Ionov, *Langmuir*, 2015, **31**, 5015–5024.
27 L. Ionov, *Mater. Today*, 2014, **17**, 494–503.
28 D. Maspoch, D. Ruiz-Molina, K. Wurst, N. Domingo, M. Cavallini, F. Biscarini, J. Tejada, C. Rovira and J. Veciana, *Nat. Mater.*, 2003, **2**, 190–195.
29 B. Seoane, S. Sorribas, Á. Mayoral, C. Téllez and J. Coronas, *Microporous Mesoporous Mater.*, 2015, **203**, 17–23.
30 J. Troyano, A. Carné-Sánchez, J. Pérez-Carvajal, L. León-Reina, I. Imaz, A. Cabeza and D. Maspoch, *Angew. Chem., Int. Ed.*, 2018, **57**, 15420–15424.
31 L. R. Parent, C. H. Pham, J. P. Patterson, M. S. Denny, S. M. Cohen, N. C. Gianneschi and F. Paesani, *J. Am. Chem. Soc.*, 2017, **139**, 13973–13976.
32 Y. Ying, Y. Cheng, S. B. Peh, G. Liu, B. B. Shah, L. Zhai and D. Zhao, *J. Membr. Sci.*, 2019, **582**, 103–110.
33 Y. Cheng, Y. Ying, S. Japip, S.-D. Jiang, T.-S. Chung, S. Zhang and D. Zhao, *Adv. Mater.*, 2018, **30**, 1802401.
34 H. Vinh-Thang and S. Kaliaguine, *Chem. Rev.*, 2013, **113**, 4980–5028.
35 J. Dechnik, J. Gascon, C. J. Doonan, C. Janiak and C. J. Sumby, *Angew. Chem., Int. Ed.*, 2017, **56**, 9292–9310.
36 M. Kalaj, K. C. Bentz, S. Ayala, J. M. Palomba, K. S. Barcus, Y. Katayama and S. M. Cohen, *Chem. Rev.*, 2020, **120**, 8267–8302.
37 X.-Y. Xie, F. Wu, X.-Q. Liu and L.-B. Sun, *Dalton Trans.*, 2019, **48**, 17153–17157.
38 J.-K. Sun, H.-J. Lin, W.-Y. Zhang, M.-R. Gao, M. Antonietti and J. Yuan, *Mater. Horiz.*, 2017, **4**, 681–687.
39 C. Prestipino, L. Regli, J. G. Vitillo, F. Bonino, A. Damin, C. Lamberti, A. Zecchina, P. L. Solari, K. O. Kongshaug and S. Bordiga, *Chem. Mater.*, 2006, **18**, 1337–1346.
40 D. Yang, Q. Jia, C. Wang and T. Zheng, *Sens. Actuators B Chem.*, 2021, **346**, 130388.
41 Y. He, J. Guo, X. Yang, B. Guo and H. Shen, *RSC Adv.*, 2021, **11**, 37744–37751.
42 X. Cai, J. Lin and M. Pang, *Cryst. Growth Des.*, 2016, **16**, 3565–3568.
43 S. Felton, M. Tolley, E. Demaine, D. Rus and R. Wood, *Science*, 2014, **345**, 644–646.
44 S. Zhuo, Z. Zhao, Z. Xie, Y. Hao, Y. Xu, T. Zhao, H. Li, E. M. Knubben, L. Wen, L. Jiang and M. Liu, *Sci. Adv.*, 2020, **6**, 1464.
45 S. Bauer, S. Bauer-Gogonea, I. Graz, M. Kaltenbrunner, C. Keplinger and R. Schwödiauer, *Adv. Mater.*, 2014, **26**, 149–162.
46 H. Zeng, P. Wasylczyk, D. S. Wiersma and A. Priimagi, *Adv. Mater.*, 2018, **30**, 1703554.
47 J.-K. Sun, W. Zhang, R. Guterman, H.-J. Lin and J. Yuan, *Nat. Commun.*, 2018, **9**, 1717.
48 W. Luo, Q. Cui, K. Fang, K. Chen, H. Ma and J. Guan, *Nano Lett.*, 2020, **20**, 803–811.
49 Z. Lei and P. Wu, *Mater. Horiz.*, 2019, **6**, 538–545.
50 C. M. Yakacki, R. Shandas, C. Lanning, B. Rech, A. Eckstein and K. Gall, *BioMater.*, 2007, **28**, 2255–2263.
51 K. Malachowski, J. Breger, H. R. Kwag, M. O. Wang, J. P. Fisher, F. M. Selaru and D. H. Gracias, *Angew. Chem., Int. Ed.*, 2014, **53**, 8045–8049.

52 G. J. Hayes, Y. Liu, J. Genzer, G. Lazzi and M. D. Dickey, *IEEE Trans Antennas Propag.*, 2014, **62**, 5416–5419.
53 J. Troyano, A. Carné-Sánchez and D. Maspoch, *Adv. Mater.*, 2019, **31**, 1808235.
54 S. Lv, L. Shuai, W. Ding, W. Ke, B. Wang and J. Wan, *Adv. Fiber Mater.*, 2021, **3**, 107–116.
55 F. Connolly, C. J. Walsh and K. Bertoldi, *Proc. Natl. Acad. Sci. U. S. A.*, 2017, **114**, 51–56.
56 Z. Hao, S. Song, B. Li, Q.-X. Jia, T. Zheng and Z. Zhang, *Sens. Actuators B Chem.*, 2022, **358**, 131448.
57 A. Legrand, Z. Wang, J. Troyano and S. Furukawa, *Chem. Sci.*, 2021, **12**, 18–33.
58 P. Falcaro, A. J. Hill, K. M. Nairn, J. Jasieniak, J. I. Mardel, T. J. Bastow, S. C. Mayo, M. Gimona, D. Gomez, H. J. Whitfield, R. Riccò, A. Patelli, B. Marmiroli, H. Amenitsch, T. Colson, L. Villanova and D. Buso, *Nat. Commun.*, 2011, **2**, 237.
59 J. Reboul, S. Furukawa, N. Horike, M. Tsotsalas, K. Hirai, H. Uehara, M. Kondo, N. Louvain, O. Sakata and S. Kitagawa, *Nat. Mater.*, 2012, **11**, 717–723.
60 R. Ameloot, L. Stappers, J. Fransaer, L. Alaerts, B. F. Sels and D. E. De Vos, *Chem. Mater.*, 2009, **21**, 2580–2582.
61 F. Cheng, E. S. Marshall, A. J. Young, P. J. Robinson, J.-S. G. Bouillard, A. M. Adawi, N. A. Vermeulen, O. K. Farha, M. R. Reithofer and J. M. Chin, *Chem. – Eur. J.*, 2017, **23**, 15578–15582.
62 S. B. Peh, A. Karmakar and D. Zhao, *Trends Chem.*, 2020, **2**, 199–213.
63 J. Troyano, A. Legrand and S. Furukawa, *Trends Chem.*, 2021, **3**, 254–265.
64 Y. Ikezoe, G. Washino, T. Uemura, S. Kitagawa and H. Matsui, *Nat. Mater.*, 2012, **11**, 1081–1085.
65 A. Ayala, C. Carbonell, I. Imaz and D. Maspoch, *Chem. Commun.*, 2016, **52**, 5096–5099.
66 Y. Yang, X. Arqué, T. Patiño, V. Guillerm, P.-R. Blersch, J. Pérez-Carvajal, I. Imaz, D. Maspoch and S. Sánchez, *J. Am. Chem. Soc.*, 2020, **142**, 20962–20967.
67 X. Zhang, P. Xue, X. Yang, C. Valenzuela, Y. Chen, P. Lv, Z. Wang, L. Wang and X. Xu, *ACS Appl. Mater. Interfaces*, 2022, **14**, 11834–11841.
68 Z. Hu, C.-a Tao, F. Wang, X. Zou and J. Wang, *J. Mater. Chem. C*, 2015, **3**, 211–216.
69 J. Zhao, L. Cheng, K. Liu, Z. Zhang, W. Yu and X. Yan, *Chem. Commun.*, 2020, **56**, 8031–8034.
70 D. Yan, Z. Wang and Z. Zhang, *Acc. Chem. Res.*, 2022, **55**, 1047–1058.
71 E. Lin, Z. Wang, X. Zhao, Z. Liu, D. Yan, F. Jin, Y. Chen, P. Cheng and Z. Zhang, *Angew. Chem., Int. Ed.*, 2022, **61**, e202117390.